Pair entanglement in dimerized spin-s chains

A. Boette, R. Rossignoli, N. Canosa, and J. M. Matera
IFLP, Departamento de Física, FCE, Universidad Nacional de La Plata, C.C. 67, La Plata (1900), Argentina
(Received 24 September 2016; revised manuscript received 14 November 2016; published 5 December 2016)

We examine the pair entanglement in the ground state of finite dimerized spin-s chains interacting through anisotropic XY couplings immersed in a transverse magnetic field by means of a self-consistent pair mean-field approximation. The approach, which makes no *a priori* assumptions on the pair states, predicts, for sufficiently low coupling between pairs, $2s$ distinct dimerized phases for increasing fields below the pair factorizing field, separated by spin-parity-breaking phases. The dimerized phases lead to approximate magnetization and pair entanglement plateaus, while the parity-breaking phases are characterized by weak pair entanglement but non-negligible entanglement of the pair with the rest of the system. These predictions are confirmed by the exact results obtained in finite $s = 1$ and $s = 3/2$ chains. It is also shown that for increasing values of the spin s, the entanglement of an isolated pair, as measured by the negativity, rapidly saturates in the anisotropic XY case but increases as $s^{1/2}$ in the XX case, reflecting a distinct single-spin entanglement spectrum.

DOI: 10.1103/PhysRevB.94.214403

I. INTRODUCTION

The study of entanglement in interacting spin systems has received strong attention in recent years [1,2]. Entanglement has provided a novel perspective for the analysis of correlations and quantum phase transitions [1–4], being also essential for determining the potential of such systems in the field of quantum information [5,6]. Interest in spin systems has been enhanced by the impressive advances in control techniques of quantum systems that have made it possible to simulate interacting spin models with different types of couplings by means of trapped ions, Josephson junctions, or cold atoms in optical lattices [7–12].

In particular, dimerized systems, characterized by strongly coupled spin pairs, are of great interest, providing a basis for understanding magnetization plateaus and nontrivial magnetic behavior [13]. The phenomenon of dimerization can arise from distinct geometric configurations and couplings [13–29], and has also been recently simulated with cold atoms in optical lattices [30]. While the basic case deals with singlet pairs in frustrated antiferromagnetic (AFM)-like systems [14,28], other types of dimerization can also arise in the ground state (GS) of systems with nonuniform couplings, like spin chains with alternating-type XYZ couplings [16–18,25–27,29]. In these systems a basic mean-field approximation (MF) based on independent spins clearly fails to provide even the most basic features of the GS and its magnetic behavior. Instead, we have shown [29] that a pair MF approach, a particular case of a generalized cluster-type variational mean-field treatment, based on independent pairs whose state is self-consistently determined and admitting relevant symmetry breaking, is able to provide a correct basic description. In dimerized spin-1/2 arrays with anisotropic XY and XYZ couplings, the approach is in fact analytic, providing a phase diagram that differs from that of the standard MF and contains a (single) dimerized phase at low fields under appropriate conditions [29]. Such a prediction is in good agreement with the exact results, which in the special case of spin-1/2 chains with first-neighbor XY couplings can be analytically obtained through the Jordan-Wigner fermionization [16,17,27,31].

The aim of this work is to extend previous results to spin-s systems with $s \geqslant 1$, which are also of interest [21–23] and where the previous fermionization is no longer available, with the system Hilbert space dimension becoming rapidly very large as the total number of spins increases. In this scenario we will show that the self-consistent pair MF approach constitutes a convenient method for understanding the basic physics, which can still depart considerably from the conventional MF prediction and the bosoniclike behavior expected for high spin [32]. The approach also provides an accurate description of the reduced state of pairs, enabling determination of the main features of the pair entanglement. In particular, for sufficiently low coupling and appropriate anisotropies, the approach predicts $2s$ dimerized phases for increasing fields below the factorizing field [26,27,33], characterized by magnetization and pair entanglement approximate plateaus, which are separated by S_z parity-breaking phases where the pair entanglement drops considerably while that of the pair with the remaining chain becomes non-negligible. These features are confirmed by the exact numerical results obtained in small finite spin-1 and -3/2 chains. We will also analyze the behavior for large spin, showing the distinct entanglement properties of anisotropic XY and XX pairs. The formalism and its application to dimerized spin-s XY systems is described in Sec. II, while results are discussed in detail in Sec. III. Conclusions are given in Sec. IV.

II. FORMALISM

A. Pair mean field in dimerized arrays and parity breaking

We consider a finite chain of $2n$ spins s in a transverse uniform field B interacting through alternating first-neighbor anisotropic XY couplings [16–18,26,27], such that the chain contains strongly coupled pairs weakly interacting with their neighboring pairs. The Hamiltonian can be written as

$$H = \sum_{i=1}^{n} \left[B\left(S^z_{2i-1} + S^z_{2i}\right) - \sum_{\mu=x,y} J_\mu \left(S^\mu_{2i-1} S^\mu_{2i} + \alpha S^\mu_{2i} S^\mu_{2i+1}\right) \right], \tag{1}$$

where S^μ_i are the spin components at site i [with $S^\mu_{2n+1} = S^\mu_1$ (0) in the cyclic (open) case], J_μ are the exchange couplings, and the parameter α indicates the relative strength of the coupling between pairs ($|\alpha| \leqslant 1$). Without loss of generality we can

assume (for even n in the cyclic case) $\alpha \geqslant 0$ and $J_x \geqslant 0$, as their signs can be changed by local rotations around the z axis, which will not alter the spectrum nor the entanglement properties of H. We can also set $|J_y| \leqslant J_x$ by conveniently choosing the x axis and $B \geqslant 0$. (Its sign is changed by a global rotation around the y axis.) The relevant symmetry for $J_y \neq J_x$ is the S^z parity

$$P_z = \exp\left[\iota\,\pi \sum_{i=1}^{2n} \left(S_i^z + s\right)\right] = \prod_{i=1}^{2n} P_{zi}, \tag{2}$$

satisfying $[P_z, H] = 0$. It implies $\langle S_i^x\rangle = \langle S_i^y\rangle = 0\ \forall i$ in any nondegenerate eigenstate of H.

In a pair mean-field treatment, the GS of (1) is approximated by a pair product state $|\Psi_0\rangle = \prod_{i=1}^{n} |\psi_{0i}\rangle$, with $|\psi_{0i}\rangle$ the state of the pair $(2i-1,2i)$. Minimization of $\langle\Psi_0|H|\Psi_0\rangle$ then leads to the independent pair self-consistent Hamiltonian $h = \sum_{i=1}^{n} h_i$, with

$$\begin{aligned} h_i = {} & B\left(S_{2i-1}^z + S_{2i}^z\right) - \sum_{\mu} J_\mu \left[S_{2i-1}^\mu S_{2i}^\mu \right. \\ & \left. + \alpha\left(\left\langle S_{2i-2}^\mu\right\rangle S_{2i-1}^\mu + \left\langle S_{2i+1}^\mu\right\rangle S_{2i}^\mu\right)\right], \end{aligned} \tag{3}$$

where $\langle S_{2i+j}^\mu\rangle = \langle\psi_{0i}|S_{2i+j}^\mu|\psi_{0i}\rangle$, $i = 1,\ldots,n$, $j = -1,0$, are the mean values in the GS $|\psi_{0i}\rangle$ of h_i: $h_i|\psi_{0i}\rangle = E_{0i}|\psi_{0i}\rangle$ (*self-consistency conditions*). The essential difference with a conventional MF is that the internal coupling of the pair is treated *exactly*. Parity breaking is still required for a nonzero average coupling between pairs, but the possibility of parity-preserving *dimerized* solutions is now open. The approximate GS energy is $\langle\Psi_0|H|\Psi_0\rangle = \sum_{i=1}^{n}[E_{0i} + \alpha\sum_\mu J_\mu\langle S_{2i}^\mu\rangle\langle S_{2i+1}^\mu\rangle]$, and in the case of several self-consistent solutions, that with the lowest energy is to be selected.

In the setting considered ($J_x > 0$, $|J_y| < J_x$, $\alpha > 0$), the pair MF of lowest energy is reached for $\langle S_i^y\rangle = 0\ \forall\ i$, since, writing $(\langle S_i^x\rangle, \langle S_i^y\rangle) = |\langle \boldsymbol{S}_i^\perp\rangle|(\cos\phi_i, \sin\phi_i)$, the MF coupling energy between adjacent pairs, $-\alpha\sum_\mu J_\mu\langle S_{2i}^\mu\rangle\langle S_{2i+1}^\mu\rangle \propto -(J_x\cos\phi_{2i}\cos\phi_{2i+1} + J_y\sin\phi_{2i}\sin\phi_{2i+1})$, is clearly minimized for $\phi_{2i} = \phi_{2i+1} = 0$ (or π) if $|J_y| < J_x$. These values of ϕ_i also minimize the internal coupling energy of the pair for fixed values of the $|\boldsymbol{S}_i^\perp|$. We have in fact verified that parity-breaking self-consistent pair MF solutions have in the present case either $\langle S_i^x\rangle \neq 0$, $\langle S_i^y\rangle = 0$, or $\langle S_i^x\rangle = 0$, $\langle S_i^y\rangle \neq 0$, but the latter never provides a lower energy. In the cyclic case we can also assume for the chosen setting a *uniform* pair mean field such that $\langle S_{2i-1}^x\rangle = \langle S_{2i}^x\rangle \equiv \langle S^x\rangle\ \forall\ i$. In the open case the site dependence of $\langle S_i^x\rangle$ should be determined self-consistently, but the solution for a uniform B will be practically uniform except for small border corrections at the endpoints.

Hence, the pair MF can be here characterized by a single parity-breaking parameter $\langle S^x\rangle$: If $\langle S^x\rangle = 0$ it leads to a parity-preserving *dimerized phase* at the pair MF level, with no average coupling between pairs, while if $\langle S^x\rangle \neq 0$ it corresponds to a *parity-breaking phase*, with nonzero coupling between pairs. This last phase is, of course, twofold degenerate for $|J_y| < J_x$, as both signs $\langle S^x\rangle = \pm|\langle S^x\rangle|$ are equally possible, with $|\psi_{0i}^-\rangle = P_{zi}|\psi_{0i}^+\rangle$. At the parity-breaking phases we will then consider the definite parity combinations

$$|\Psi_{0\pm}\rangle \propto (\mathbb{1} \pm P_z)\prod_{i=1}^{n}|\psi_{0i}^+\rangle = \prod_{i=1}^{n}|\psi_{0i}^+\rangle \pm \prod_{i=1}^{n}|\psi_{0i}^-\rangle, \tag{4}$$

which satisfy $P_z|\Psi_{0\pm}\rangle = \pm|\Psi_{0\pm}\rangle$ and correctly lead to $\langle S_i^x\rangle = 0\ \forall\ i$, selecting that of lower energy. Note that these states possess a *finite* entanglement between pairs.

B. Critical conditions

In order to determine the onset of parity breaking, we may consider the first-order expansion of the common pair ground state $|\psi_0\rangle = |\psi_{0i}\rangle$ for small $\langle S^x\rangle$, $|\psi_0\rangle \approx |\psi_0^0\rangle + |\delta\psi_0\rangle$, where $|\delta\psi_0\rangle = \alpha J_x\langle S^x\rangle\sum_{k>0}\frac{\langle\psi_k^0|S_t^x|\psi_0^0\rangle}{E_k - E_0}|\psi_k^0\rangle$, with $S_t^x = S_1^x + S_2^x$ and $\{|\psi_k^0\rangle\}$ the eigenstates of the $\langle S^x\rangle = 0$ pair Hamiltonian h^0: $h^0|\psi_k^0\rangle = E_k|\psi_k^0\rangle$. Since pair parity symmetry, exactly conserved in h^0, implies $\langle\psi_0^0|S_t^x|\psi_0^0\rangle = 0$ (assuming $|\psi_0^0\rangle$ nondegenerate) we have $\langle S^x\rangle \approx \mathrm{Re}[\langle\psi_0^0|S_t^x|\delta\psi_0\rangle]$ up to first order in $\langle S^x\rangle$, implying the critical condition

$$1 = \alpha J_x \sum_{k>0} \frac{\left|\left\langle\psi_k^0\right|S_t^x\left|\psi_0^0\right\rangle\right|^2}{E_k - E_0}. \tag{5}$$

Parity breaking is then feasible if

$$\alpha > \alpha_c = \frac{1}{J_x\sum_{k>0}\frac{\left|\left\langle\psi_k^0\right|S_t^x\left|\psi_0^0\right\rangle\right|^2}{E_k - E_0}}. \tag{6}$$

Equation (6) determines a *finite* threshold value α_c for parity breaking whenever the isolated pair is *gapped* ($E_k - E_0 > 0\ \forall\ k > 0$), which will depend on the relative field strength B/J_x, the ratio $\chi = J_y/J_x$, and the spin s. The sum in (5) is typically exhausted by the first term $\frac{|\langle\psi_1^0|S_t^x|\psi_0^0\rangle|^2}{E_1 - E_0}$, where E_1 is the lowest energy of S^z parity opposite to that of E_0. The restriction $\alpha \leqslant 1$ sets also an upper bound on B/J_x for parity breaking ($B < B_c^p$).

On the other hand, the threshold value α_c in (6) *vanishes* when the smallest excitation energy $E_1 - E_0$ becomes zero. Hence, pair GS transitions (level crossings) arising for increasing fields will originate parity-breaking phases for finite $\alpha > 0$ *even if* α *is small*, in which the coupling between pairs cannot be treated perturbatively. For small α they will emerge between *distinct* dimerized phases. Hence, several onsets (followed by "deaths") of parity breaking as the field increases can take place, as will be shown in the next section. For $s = 1/2$ there are in fact *two* parity-preserving phases for increasing fields if $\chi > 0$ and $\alpha < \frac{1}{2}\chi$ [29], separated by a *single* parity-breaking window $B_{c1} < B < B_{c2}$.

Such multiple dimerized phases are absent for any spin s in the conventional single-spin MF (full product state approximation), which in this system becomes equivalent to the MF treatment of a standard chain with uniform coupling of strength $J_x(1+\alpha)/2$, being independent of J_y if $|J_y| < J_x$. For any spin s it leads to a single parity-breaking phase for $0 \leqslant |B| < B_c^{\mathrm{mf}} \equiv J_x s(1+\alpha)$, where $\langle S^x\rangle = \pm s\sin\theta$ with $\cos\theta = B/B_c^{\mathrm{mf}}$. The pair MF phase diagram will become similar to that of the conventional MF for large α, although the upper critical field for parity breaking will be slightly smaller [29] (see next section).

Nevertheless, for $0 < J_y < J_x$ there is one point where *both* the single-spin and pair mean-field treatments exactly coincide and become rigorously *exact* for *any* value of the spin s and the number n of spins, i.e., where the chain GS completely forgets its dimerized structure, which is the *factorizing field* [26,27,29,33]

$$B_s = J_x s(1+\alpha)\sqrt{\chi}, \quad \chi = J_y/J_x. \tag{7}$$

At this field the chain exhibits a pair of degenerate *completely separable* parity-breaking aligned ground states

$$|\pm\Theta\rangle = |\pm\theta, \pm\theta, \ldots\rangle, \tag{8}$$

with $|\pm\theta\rangle = e^{\mp i\theta S^y}|-s\rangle$ a single-spin state with maximum spin, forming an angle $\pm\theta$ with the $-z$ axis, with $\cos\theta = B_s/B_c^{\rm mf} = \sqrt{\chi}$. In a finite chain the factorizing field (7) is actually that where the *last* GS parity transition takes place [34,35] (see next section). Accordingly, the one-sided left and right limits of the exact GS at B_s in a finite chain will not be given by the product states (8) but rather by the definite parity combinations $|\Theta_\pm\rangle \propto |\Theta\rangle \pm |-\Theta\rangle$, with $P_z|\Theta_\pm\rangle = \pm|\Theta_\pm\rangle$ [34,35], which will be correctly predicted by the symmetry-restored pair MF states (4). A GS transition $|\Theta_-\rangle \to |\Theta_+\rangle$ will then take place as B crosses B_s.

For AFM-type couplings [$J_x < 0$ and/or $\alpha < 0$ in (1)], factorizing and critical values of B and $|\alpha|$ will take exactly the same previous values (with $J_x \to |J_x|$, $\alpha \to |\alpha|$). Just suitable local rotations are to be applied to the corresponding state, as previously mentioned. For instance, if $J_x > 0$ but $\alpha < 0$, they will transform the previous uniform pair state into a Néel-type pair state $|\Psi_0\rangle = |\psi_0\rangle|\tilde{\psi}_0\rangle|\psi_0\rangle\ldots$ with $|\tilde{\psi}_0\rangle = e^{\imath\pi(S_1^z+S_2^z)}|\psi_0\rangle \propto P_z|\psi_0\rangle$ and $\langle S^x\rangle_{2i+j} = (-1)^{i-1}\langle S^x\rangle$ for $j = 0, -1$. These rotations will not affect entanglement measures.

The pair MF approach can, of course, be also applied to more complex couplings and geometries. For instance, if the coupling between pairs i and $i+1$ contains second- and third-neighbor terms, i.e., $-\sum_\mu J_\mu \sum_{j,l=1,2} \alpha_{jl} S^\mu_{2i-2+j} S^\mu_{2i+l}$, we should just replace the α term in (3) by $\sum_{j,l=1,2} S^\mu_{2i-2+j}(\alpha_{jl}\langle S^\mu_{2i+l}\rangle + \alpha_{lj}\langle S^\mu_{2i-4+l}\rangle)$. If translational symmetry remains unbroken, as will occur for $\alpha_{11} = \alpha_{22}$ and all $\alpha_{jl} \geqslant 0$, previous equations can be directly applied, leading to the same critical condition (5) with α replaced by $\sum_{j,l}\alpha_{jl}$.

C. Entanglement

The reduced state of a strongly coupled pair in the exact GS $|\Psi_0\rangle$ of the chain is given by $\rho_{12} = {\rm Tr}_{3,4,\ldots}|\Psi_0\rangle\langle\Psi_0|$. The entanglement of the pair with the rest of the chain can be measured through the entanglement entropy $S(\rho_{12}) = -{\rm Tr}\rho_{12}\log_2\rho_{12}$, satisfying $S(\rho_{12}) \leqslant 2\log_2(2s+1)$ for a pair of spins s. On the other hand, its internal entanglement can be estimated through the negativity (an entanglement monotone computable for mixed states of any dimension [36,37])

$$N_{12} = \left({\rm Tr}\left|\rho_{12}^{t_2}\right| - 1\right)/2, \tag{9}$$

where $\rho_{12}^{t_2}$ denotes the partial transpose of ρ_{12}. Equation (9) is just minus the sum of the negative eigenvalues of $\rho_{12}^{t_2}$. If ρ_{12} is pure, Eq. (9) becomes a generalized entanglement entropy,

$$N_{12} = [({\rm Tr}\sqrt{\rho_1})^2 - 1]/2 = \sum_{i<j}\lambda_i^1\lambda_j^1, \tag{10}$$

where $\rho_1 = {\rm Tr}_2\,\rho_{12} = {\rm Tr}_2\,|\psi_0\rangle\langle\psi_0|$ is the single-spin reduced state and λ_i^1 its eigenvalues. Accordingly, Eq. (10) vanishes for ρ_1 pure ($|\psi_0\rangle$ separable) and reaches its maximum for a maximally mixed ρ_1 ($|\psi_0\rangle$ maximally entangled), in which case $N_{12} = s$ for a pair of spins s.

At the pair MF level, ρ_{12} will be pure in the parity-preserving phases. However, in the parity-breaking phases ρ_{12} will become *mixed* if the parity-restored states (4) are employed. The latter leads to a rank-2 reduced state of the form

$$\rho_{12} \approx \tfrac{1}{2}(|\psi_0^+\rangle\langle\psi_0^+| + |\psi_0^-\rangle\langle\psi_0^-|), \tag{11}$$

if the complementary overlap $|\langle\psi_0^+|\psi_0^-\rangle|^{n-1}$ (negligible if n and $\langle S^x\rangle$ are not too small) is discarded, whose nonzero eigenvalues are just $\lambda_\pm = \frac{1}{2}(1 \pm |\langle\psi_0^-|\psi_0^+\rangle|)$. Hence, a nonzero entanglement entropy of the pair with the rest of the chain will arise at the pair MF level within the parity-breaking phases, which will then satisfy $S(\rho_{12}) \leqslant 1$, with $S(\rho_{12}) \approx 1$ if the overlap $\langle\psi_0^-|\psi_0^+\rangle$ is also negligible.

At the factorizing field (7), Eq. (11) becomes *exact* (if $\langle-\theta,-\theta|\theta,\theta\rangle^{n-1} = (\cos^{4s}\theta)^{n-1}$ is neglected), with $|\psi_0^\pm\rangle = |\pm\theta, \pm\theta\rangle$ product states. Consequently, even with symmetry restoration the exact one-sided limits of ρ_{12} at B_s will become *separable*, i.e., a convex combination of product states [38], leading to $N_{12} = 0$ at this point. Nonetheless, it will remain *mixed*, with eigenvalues $\lambda_\pm = \frac{1}{2}(1 \pm \cos^{4s}\theta)$, implying a nonzero entanglement of the pair with the rest of the chain at the left- and right-hand limits $B \to B_s^\pm$.

III. RESULTS

A. The spin-1 case

1. The spin-1 pair

We first examine in detail the case $s = 1$. In order to understand the behavior of both the pair MF and the exact solution for general α in (1), we first discuss the isolated pair ($\alpha = 0$). The lowest energy levels of the pair for each parity P_z and for $|J_y| \leqslant J_x$ are

$$E_+ = -\sqrt{2B^2 + \frac{J_x^2+J_y^2}{2} + \sqrt{4B^2(B^2 - J_xJ_y) + \frac{\left(J_x^2+J_y^2\right)^2}{4}}}, \tag{12}$$

$$E_- = -\left[\frac{J_x+J_y}{2} + \sqrt{B^2 + \frac{(J_x-J_y)^2}{4}}\right], \tag{13}$$

with eigenstates

$$|\psi_+\rangle = \alpha_-|-1,-1\rangle + \alpha_0|0,0\rangle + \alpha_+|1,1\rangle + \alpha_{11}\frac{|-1,1\rangle + |1,-1\rangle}{\sqrt{2}}, \tag{14}$$

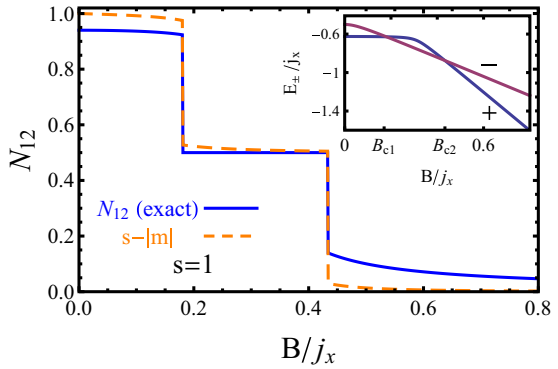

FIG. 1. Negativity of the spin-1 pair GS for an anisotropic XY coupling with $\chi = J_y/J_x = 0.75$, as a function of the scaled transverse field B/j_x, with $j_x = 2J_x s$. The quantity $s - |m|$, with m the intensive magnetization $\langle S_1^z + S_2^z\rangle/2$, is also depicted. The inset depicts the lowest energy levels $E_\pm$ for each parity, which cross at B_{c1} and $B_{c2} = B_s$ (pair separability field) and lead to the negativity steps (all labels dimensionless in all figures).

$$|\psi_-\rangle = \beta_- \frac{|-1,0\rangle + |0,-1\rangle}{\sqrt{2}} + \beta_+ \frac{|0,1\rangle + |1,0\rangle}{\sqrt{2}} = \frac{|0,\phi\rangle + |\phi,0\rangle}{\sqrt{2}}, \quad (15)$$

in the standard product basis $\{|m_1,m_2\rangle\}$ of eigenstates of S_1^z and S_2^z, where

$$\alpha_0 = \alpha_- \frac{2(|E_+| - 2B)}{J_x - J_y}, \quad \alpha_+ = \alpha_- \frac{|E_+| - 2B}{|E_+| + 2B},$$
$$\alpha_{11} = \alpha_0 \frac{J_x + J_y}{\sqrt{2}|E_+|},$$
$$\beta_+ = \beta_- \frac{2(|E_-| - B) - (J_x + J_y)}{J_x - J_y}. \quad (16)$$

Here $|\psi_-\rangle$ is seen to be a Bell-type state, with $|\phi\rangle = \beta_-|-1\rangle + \beta_+|1\rangle$, whereas $|\psi_+\rangle$ has full Schmidt rank if $J_y \neq J_x$. For strong fields $B \gg J_x$, $E_+ \approx -2B$, $E_- \approx -B$, while for zero field $E_+ = -J_x\sqrt{1+\chi^2}$, $E_- = -J_x$, so that $|\psi_+\rangle$ is the GS in these limits. Yet if $\chi = J_y/J_x \in (0,1]$, $|\psi_-\rangle$ will be the GS in an intermediate field window $B_{c1} \leqslant B \leqslant B_{c2}$, as seen in the inset of Fig. 1, with

$$B_{c1} \approx \sqrt{\chi} J_x \frac{(1 - 4\chi/25)}{\sqrt{5}}, \quad B_{c2} = \sqrt{\chi} J_x = B_s, \quad (17)$$

where the expression for B_{c1} holds for small χ and B_s is the *separability field* (7) for the isolated pair ($\alpha = 0$). Hence, for $\chi > 0$ the pair GS will undergo two parity transitions as the field increases from 0, the last one at B_s. These transitions are reminiscent of the magnetization transitions $M \to M - 1$ for $M = 0,1$ of the XX case $J_y = J_x$ ($\chi = 1$), where the eigenvalue M of $S_t^z = S_1^z + S_2^z$ is a good quantum number and $B_{c1} = (\sqrt{2} - 1)J_x$, $B_s = J_x = B_c^{\rm mf}$. Accordingly, in the XX case the eigenstates (14)–(15) become $|\psi_+\rangle = \frac{1}{\sqrt{2}}(\frac{|-1,1\rangle+|1,-1\rangle}{\sqrt{2}} + |0,0\rangle)$ for $|B| < B_{c1}$ and $|-1,-1\rangle$ for $B > B_s$, with $|\psi_-\rangle = \frac{|-1,0\rangle+|0,-1\rangle}{\sqrt{2}}$. Here GS separability holds $\forall\, B \geqslant B_s$.

In both the XY and XX cases, these GS transitions lead to a stepwise decrease of the pair entanglement, which parallels that of $s - |m|$, with $m = \langle S_t^z\rangle/2$ the intensive magnetization, as seen in Fig. 1. Since $|\psi_-\rangle$ is a Bell-type state, it has a *fixed* entanglement entropy $S_{12} = 1$ and negativity $N_{12} = 1/2$, independent of the anisotropy and field intensity (strict entanglement plateau). On the other hand, $|\psi_+\rangle$ in (14) leads to a larger negativity for $|B| < B_{c1}$, not strictly constant, given at zero field by

$$N_{12} = \frac{1 + |\chi|(1 + |\chi| + \chi^2 + \sqrt{1+\chi^2})}{2\sqrt{(1+\chi^2)^3}}. \quad (18)$$

This value increases with $|\chi|$ for $|\chi| \leqslant 1$, reaching $N_{12} = \frac{1}{4} + \frac{1}{\sqrt{2}} \approx 0.96$ at $\chi = 1$ (close to the maximum value $N_{12}^{\max} = 1$ for a spin-1 pair). In contrast, for strong fields $|B| > B_s$ the state (14) becomes almost aligned, with just α_- remaining significant, implying a small negativity $N_{12} \approx \frac{J_x(1-\chi)}{4B}$. As previously stated, it is clearly seen that the one-sided limits of the GS at the pair factorizing field $B_{c2} = B_s$ are the entangled states $|\psi_\pm\rangle$, which at this point become linear combinations of the separable states $|\pm\theta,\pm\theta\rangle$ [Eq. (8)].

The average magnetization $\langle S_t^z\rangle$ is given by $\beta_+^2 - \beta_-^2 = \frac{-B}{\sqrt{B^2 + J_x^2(1-\chi)^2/4}}$ in $|\psi_-\rangle$, which is close to -1 in the sector where it is GS, and by $2(\alpha_+^2 - \alpha_-^2)$ in $|\psi_+\rangle$, becoming $\approx -\frac{B(1-\chi)^2}{J_x(1+\chi^2)^{3/2}}$ for weak fields $|B| < B_{c_1}$ and $\approx \frac{J_x^2(1-\chi)^2}{8B^2} - 2$ for strong fields $B > B_s$. Hence, the behavior of $s - |m|$ resembles that of the negativity, with $s - |m| \approx N_{12}^2$ for strong fields.

2. The spin-1 chain

Returning now to the coupled spin-1 chain, the previous GS transitions of the isolated pair will imply three distinct dimerized phases if $\chi > 0$ and α is sufficiently small, as seen in the pair MF phase diagram depicted in Fig. 2. For fixed $B < B_c^p \approx J_x s$, Eq. (6) determines the threshold value $\alpha_c(B)$ for parity breaking, which vanishes precisely at the critical fields B_{c1} and B_{c2} of the isolated pair. For $\alpha < \alpha_c(B)$ we then obtain a *dimerized phase* in this approach, with all strongly coupled pairs in a strongly entangled state $|\psi_+\rangle$ [Eq. (14)] if $|B| < B_{c1}$ or $|\psi_-\rangle$ [Eq. (15)] if $B_{c1} < B < B_s$, and back to an almost aligned state $|\psi_+\rangle$ if $B > B_s$. As B increases from 0 at fixed small α, the pair MF state can then undergo *four* transitions between definite parity and parity-breaking phases or vice versa, as shown in Fig. 2. At zero field, Eq. (6) leads to the critical value

$$\alpha_c(0) = (1+\chi^2)[\sqrt{1+\chi^2}(4+\chi^2) - 4 - 3\chi^2]/\chi^4, \quad (19)$$

which increases with $|\chi|$, reaching $\sim$0.14 for $|\chi| \to 1$ and vanishing as $\sim\chi^2/8$ for $\chi \to 0$. For $\chi = 0.75$ (Fig. 2), $\alpha_c(0) \approx 0.077$.

On the other hand, if $\alpha > \alpha_c(0)$ we obtain a single parity-breaking phase for $|B| < B_c(\alpha)$, with $B_c(\alpha)$ lying between the factorizing field (7) and the standard MF critical field $B_c^{\rm mf}$, as also seen in Fig. 2. In the XX limit $\chi = 1$, $B_s(\alpha) = B_c(\alpha) = B_c^{\rm mf}(\alpha) = J_x$. We also mention that if $\chi < 0$ ($-J_x < J_y < 0$),

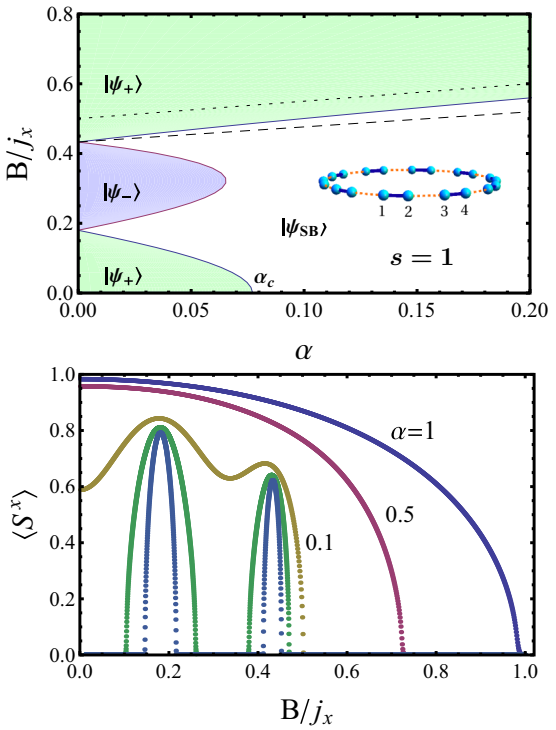

FIG. 2. Top: Pair mean-field (GMF) phase diagram of the spin-1 dimerized cyclic chain in the α-field plane for $\chi = J_y/J_x = 0.75$. Colored sectors depict dimerized definite S_z parity phases ($\langle S^x \rangle = 0$), whereas the white sector corresponds to the parity-breaking phase [α_c indicates the critical value (19) at zero field]. The dashed line depicts the separability field (7), entirely contained in the parity-breaking phase, which determines the last parity transition of the exact GS. The dotted line indicates the conventional mean-field critical field $B_c^{\rm mf} = J_x s(1+\alpha)$. Bottom: The parity-breaking parameter $\langle S^x \rangle$ for increasing fields at different fixed α's (0.025, 0.05, 0.1, 0.5, and 1). Its behavior reflects the phases of the top panel, showing a nonmonotonous field dependence at low α, with "deaths and revivals" if $\alpha < \alpha_c$. For $\alpha = 1$ it lies close to the conventional MF result.

the isolated pair remains gapped for all fields, with a GS which is always of positive parity and exhibits no sharp transitions. Consequently, in this case parity breaking occurs just above a *finite* threshold $\alpha_c(B) > \alpha_c(0)\ \forall\ B < B_c^p$, i.e., for $\alpha > \alpha_c(0)$ and $|B| < B_c(\alpha) < B_c^{\rm mf}(\alpha)$. If $\alpha < \alpha_c(0)$ and $\chi < 0$ no parity breaking occurs. Thus, we see that the weaker strength J_y does strongly affect the pair MF phase diagram, in contrast with the single-spin MF.

Figure 3 depicts in the top-left panel results for the exact negativity of a strongly coupled pair for increasing fields at fixed low $\alpha = 0.05$ and $\chi = 0.75$, together with the intensive magnetization $m = \langle \sum_i S_i^z \rangle/(2n)$ (through the quantity $s - |m|$), obtained numerically by means of diagonalization in a small cyclic chain of $2n = 8$ spins. It is first seen that the pair MF prediction, denoted in what follows as GMF (generalized mean field), is in very good agreement with the exact results. The two dimerized phases for $B < B_s$ lead to corresponding approximate plateaus in the negativity N_{12} and magnetization. In the parity-breaking phases, N_{12} drops considerably, with the GMF result remaining accurate if evaluated with the parity-restored mixed state (11). The vanishing of N_{12} at the factorizing field $B_s \approx 0.45\, j_x$ is also observed. The behavior of $s - |m|$, on the other hand, is close to that of the pair negativity but exhibits just a straight decrease at the parity-breaking sectors, reflecting actually the behavior of the single-spin entanglement entropy S_1, shown in the bottom panel.

On the right panels we depict results for $\alpha = 0.1$, for which the definite parity-dimerized phases are no longer present in GMF, yet the order parameter $\langle S^x \rangle$ still exhibits a nonmonotonous evolution with the field magnitude (Fig. 2). Accordingly, the exact results still show a nonmonotonous evolution of the negativity, in agreement with the GMF prediction. The magnetization plateaus start to disappear, with m again correctly predicted by GMF.

The magnetic behavior of the entanglement entropies of a strongly coupled spin pair [$S_2 = S(\rho_{12})$] and a single spin [$S_1 = S(\rho_1)$] with the rest of the chain are depicted in the bottom panels. That of S_2 is quite different from S_1, exhibiting peaks at the GMF parity-breaking phases or in general at the maxima of the GMF parity-breaking parameter $\langle S^x \rangle$, reflecting its behavior. Parity breaking is then directly indicative of the entanglement of the pair with the rest of the chain. Dimerization is also evident through the lower (rather than larger, as in a standard chain) value of S_2 in comparison with S_1 for most fields, except in the vicinity of the factorizing field B_s. The behavior of S_1, on the other hand, is qualitatively similar to that of $s - |m|$, since the latter is here an indicator of the mixedness of the reduced state ρ_1 as $\langle S_i^x \rangle = \langle S_i^y \rangle = 0$ due to parity symmetry. The GMF results [obtained with the mixed state (11) in parity-breaking phases] are again in good agreement with the exact results for both values of α, providing a clear interpretation and correctly predicting the maximum value $S_2^{\rm max} \approx 1$ in the parity-breaking phases. They also yield the exact one-sided limits of these entropies at the factorizing field B_s.

Moreover, the exact GS of the full chain exhibits $2ns$ parity transitions as the field increases from 0 for $\chi > 0$, again reminiscent of the $2ns$ magnetization transitions of the XX chain, with the last one precisely at the factorizing field (7). These transitions *are seen to be confined within the symmetry-breaking sectors of the GMF approach*, as shown in the top panel of Fig. 4 and in the inset of the bottom-left panel in Fig. 3. (They lead to small but appreciable discontinuities in all depicted quantities for small n.) They indicate the crossings of the lowest negative and positive parity exact energy levels, which lie very close in the parity-breaking sectors of the pair MF approach, as verified in Fig. 4.

The pair MF approach also remains quite reliable for larger values of α, providing very good results for observables such as the pair negativity, even for $\alpha = 1$ (uniform couplings), as seen in the bottom panel of Fig. 4. This result shows that pair MF can improve conventional MF results (which lead to a zero negativity at all fields) even for standard (nondimerized) chains. The pair MF transitions at fixed field from the dimerized to the parity-breaking phase for low increasing α, as well as the parity transitions of the exact GS, can also be observed, together with the vanishing of N_{12} at the factorizing value $\alpha \approx 0.15$ for $B/j_x = 0.5$. We remark finally that completely similar results are obtained in an open chain, with just small corrections for $\langle S_i^x \rangle$ at the border pairs.

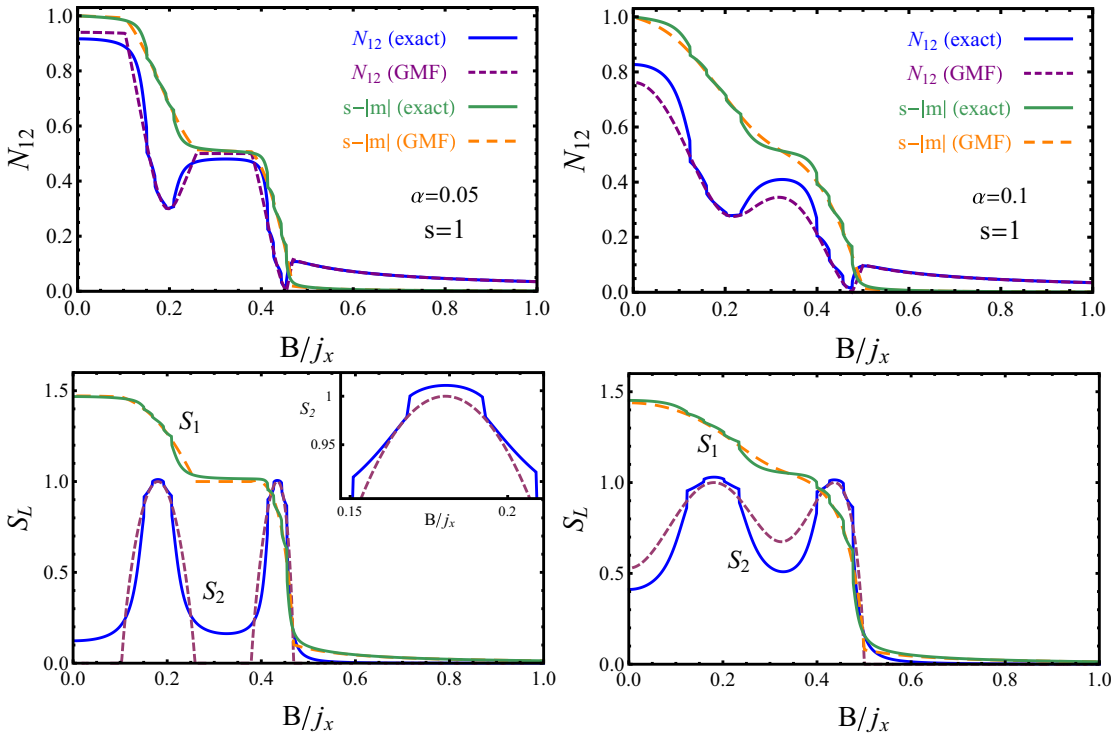

FIG. 3. Top panels: Exact and GMF results for the negativity of a strongly coupled pair in the dimerized spin-1 chain, as a function of the magnetic field, for $\chi = 0.75$ and coupling factors $\alpha = 0.05$ (left) and $\alpha = 0.1$ (right). The quantity $s - |m|$, with $m = \langle \sum_i S_i^z \rangle / 2n$ the intensive magnetization, is also depicted. Bottom panels: The corresponding exact (solid lines) and GMF (dashed lines) results for the entanglement entropies of a strongly coupled spin pair (S_2) and a single spin (S_1) with the rest of the chain, for the same values of α and s. The inset shows the discontinuities in the exact S_2 stemming from the GS parity transitions, which occur within the parity-breaking phases of the GMF approach.

B. Higher spins

1. The spin-s case

The general picture remains similar for higher spins s, but the number of definite parity-dimerized phases at fixed low α arising for $\chi > 0$ and $B < B_s$ in the pair mean field becomes $2s$, following the $2s$ GS parity transitions of the isolated pair for increasing fields (the last one at the factorizing field for the pair, $B_s = J_x s\sqrt{\chi}$). Consequently, there are three such phases for $s = 3/2$ and $B < B_s$, two of negative parity, as seen in Fig. 5. [For easier comparison between different spins, we scaled the fields with $j_x = 2J_x s$ in all figures, such that B_s/j_x and $B_c^{\rm mf}/j_x = (1+\alpha)/2$ are spin independent, with $B_c^{\rm mf}/j_x = 1$ in the uniform ($\alpha = 1$) chain.] For sufficiently small α the pair MF GS can then undergo, for $s = 3/2$, up to six transitions between definite parity and parity-breaking phases (or vice versa) as B increases.

It is also seen that the limit value of α for the existence of multiple dimerized phases for $\chi > 0$ decreases with increasing spin. At zero field, we have essentially $\alpha_c(0) \propto \Delta E/(J_x s^2)$, with $\Delta E = E_1 - E_0$ the energy gap to the first excited state. For $\chi = 1$ (XX case) $\Delta E \propto J_x$ and hence $\alpha_c(0) \propto s^{-2}$. For $s = 3/2$ we obtain in fact $\alpha_c(0) \approx 0.06$. However, for $\chi < 1$ $\alpha_c(0)$ it becomes exponentially small for large s, since now ΔE decreases exponentially with increasing spin. The behavior of $\alpha_c(B)$ with s for other fields $B < B_s$ is qualitatively similar. For $\chi = 0.75$ and $s = 3/2$ we obtain $\alpha_c(0) \approx 0.019$, as seen in Fig. 5. Nevertheless, for α above but close to $\alpha_c(0)$ the GMF parity-breaking parameter $\langle S^x \rangle$ continues to exhibit a nonmonotonous evolution for increasing fields, as seen for $\alpha = 0.05$, where it still has three local minima reminiscent of the dimerized phases. On the other hand, for $\chi < 0$ there is no parity breaking if $\alpha < \alpha_c(0)$, as in the $s = 1$ case.

The agreement of the GMF predictions with the exact numerical results remains high at small values of α, as seen in Fig. 6. The exact negativity N_{12} and pair entanglement entropy S_2 exhibit, accordingly, a nonmonotonous evolution for increasing fields at low α, with N_{12} showing for $\alpha = 0.01$ $2s$ approximate plateaus at the GMF dimerized phases separated by deep valleys at the parity-breaking sectors, before reaching the strong-field regime for $B > B_s$. On the other hand, S_2 is again maximum and close to 1 at the center of the parity-breaking phases, in full agreement with the GMF result obtained with the parity-restored states (11). We also see the $2s$ approximate magnetization plateaus, as predicted by GMF.

These effects become attenuated for $\alpha = 0.05$ (right panels), where the fully dimerized phases for $B < B_s$ no longer exist in GMF, although the behavior of N_{12} and S_2 remains nonmonotonous, in agreement with that of $\langle S^x \rangle$ in GMF. It is also seen that the GMF predictions for the magnetization and the single-spin entanglement entropy S_1 are very accurate in both panels, with $s - |m|$ a good qualitative indicator of the latter. The exact GS of the finite chain still exhibits $2ns$ parity transitions as B increases from 0, the last one at the factorizing field (7), although the ensuing discontinuities in the depicted quantities become small as s increases. They are again confined to the parity-breaking sectors of GMF (i.e., to

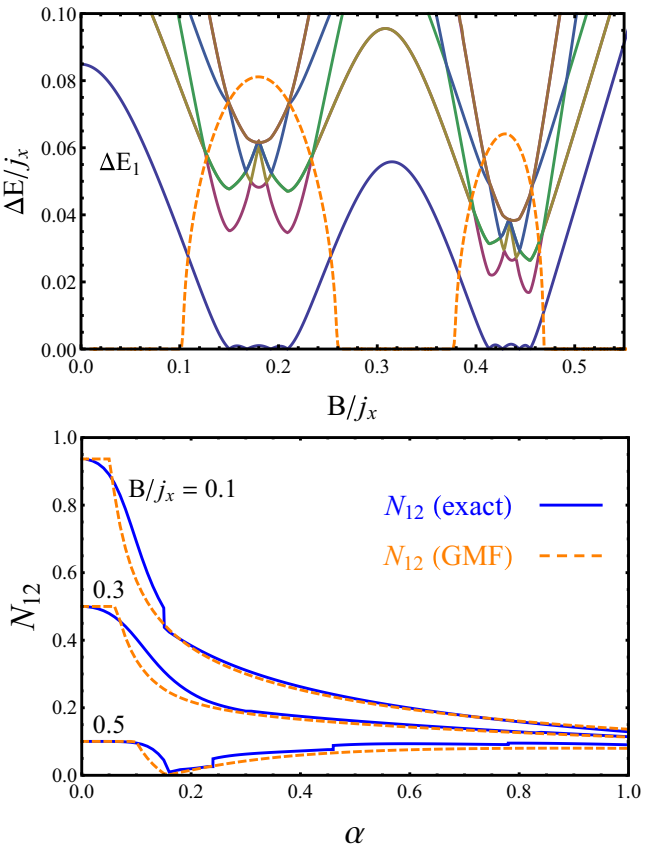

FIG. 4. Top: The lowest exact excitation energies in the $2n = 8$ dimerized spin-1 chain for $\alpha = 0.05$ and $\chi = 0.75$. The dashed line depicts the (scaled) GMF parity-breaking parameter $\langle S^x \rangle$. All parity transitions of the GS are seen to take place within the GMF parity-breaking phases, where the lowest excitation energy becomes small (and the first band of excitation energies minimum). Bottom: The negativity of a strongly coupled pair as a function of the coupling factor α at different fields for the same χ, according to exact and GMF results.

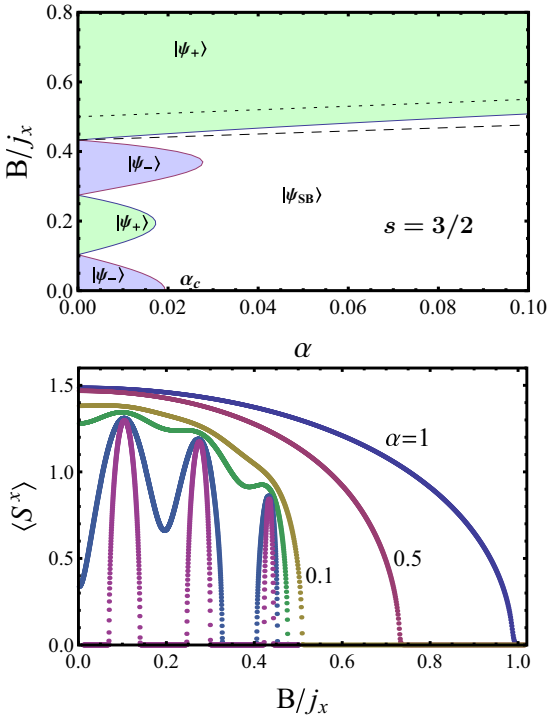

FIG. 5. Top panel: The GMF phase diagram of the spin-3/2 dimerized chain in the α-field plane for anisotropy $\chi = J_y/J_x = 0.75$. There are now three definite parity-dimerized phases below B_s (colored sectors) if α is sufficiently small. Remaining details as in Fig. 2. Bottom panel: The corresponding parity-breaking parameter $\langle S^x \rangle$ for increasing fields at different fixed values of α ((0.01, 0.02, 0.05, 0.1, 0.5, and 1). Its behavior reflects the phases of the top panel, exhibiting a nonmonotonous variation at low α, with "deaths and revivals" if $\alpha \leqslant \alpha_c(0)$.

the narrow parity-breaking intervals for $\alpha = 0.01$). As before, factorization at B_s is reflected in the vanishing value of N_{12} at this point, while the entanglement entropies S_1 and S_2 approach the finite limits determined by the corresponding state (11), with $S_2 > S_1$ only in the vicinity of B_s.

2. *Behavior for large spin*

Let us now examine in more detail the entanglement of a single isolated pair for increasing spin s. In the top panel of Fig. 7 the entanglement spectrum (the eigenvalues of the single-spin reduced density matrix ρ_1) is depicted as a function of the applied field for different spins. For $\chi < 1$ the reduced states become essentially rank-2 states as s increases in the whole sector $B < B_s$. The reason is that the main component of the pair GS ($|\psi_+\rangle$ or $|\psi_-\rangle$) is just a parity-projected rank-2 mean-field state $|\Theta_\pm\rangle$, i.e., $|\psi_\pm\rangle = \gamma|\Theta_\pm\rangle + |\delta\psi_\pm\rangle$, with

$$|\Theta_\pm\rangle = \frac{|\theta,\theta\rangle \pm |-\theta,-\theta\rangle}{\sqrt{2(1 \pm \cos^{4s}\theta)}} = \sqrt{p_\pm}|\theta_+\theta_\pm\rangle + \sqrt{1-p_\pm}|\theta_-\theta_\mp\rangle, \quad (20)$$

where the last expression is its Schmidt decomposition, with $|\theta_\pm\rangle = \frac{|\theta\rangle \pm |-\theta\rangle}{\sqrt{2(1\pm\cos^{2s}\theta)}}$ the local orthogonal definite parity states and $p_- = \frac{1}{2}$, $p_+ = \frac{(1+\cos^{2s}\theta)^2}{2(1+\cos^{4s}\theta)}$. These states lead to a rank-2 ρ_1 with eigenvalues $(p_\pm, 1-p_\pm)$. By optimizing the angle θ it is found that the overlap $|\gamma| = |\langle\Theta_\pm|\psi_\pm\rangle|$ exceeds 0.9 for all field and spin values, with $|\langle\Theta_\pm|\psi_\pm\rangle| \gtrsim 0.95$ for all fields if $s \geqslant 5$. The states (20) become, of course, the *exact* pair GS at the factorizing field B_s, with the overlap staying above 0.99 for $B > B_s$. We can verify from Fig. 7 that the contribution of $|\delta\psi_\pm\rangle$ to the entanglement spectrum is negligible.

Nonetheless, its contribution to the negativity is important if χ is not too small. For $|B| < B_s$ the states $|\Theta_\pm\rangle$ lead essentially to an almost constant negativity $N_\pm \approx 1/2$ for large s if θ is not too small, i.e., $N(|\Theta_+\rangle) = \frac{1-\cos^{4s}\theta}{2(1+\cos^{4s}\theta)}$, $N(|\Theta_-\rangle) = \frac{1}{2}$, which for $B < B_s$ lies below the exact value. The latter remains, however, *bounded as the spin s increases* if $|\chi| < 1$. Its maximum at zero field is in fact attained at low finite spin ($s \approx 2$ for $\chi = 0.75$, as seen in the bottom-left panel of Fig. 7).

For large s and $\chi < 1$, the correction $|\delta\psi_\pm\rangle$ and its effect on the pair negativity and entanglement entropy can be determined through a bosonic RPA (random phase approximation) approach [32]. Around the normal mean-field phase ($B > B_c = J_x s$), such an approach implies at lowest order the replacements $S_i^z \approx b_i^\dagger b_i - s$, $S_i^+ \approx b_i^\dagger$, $S_i^- \approx b_i$, with b_i,

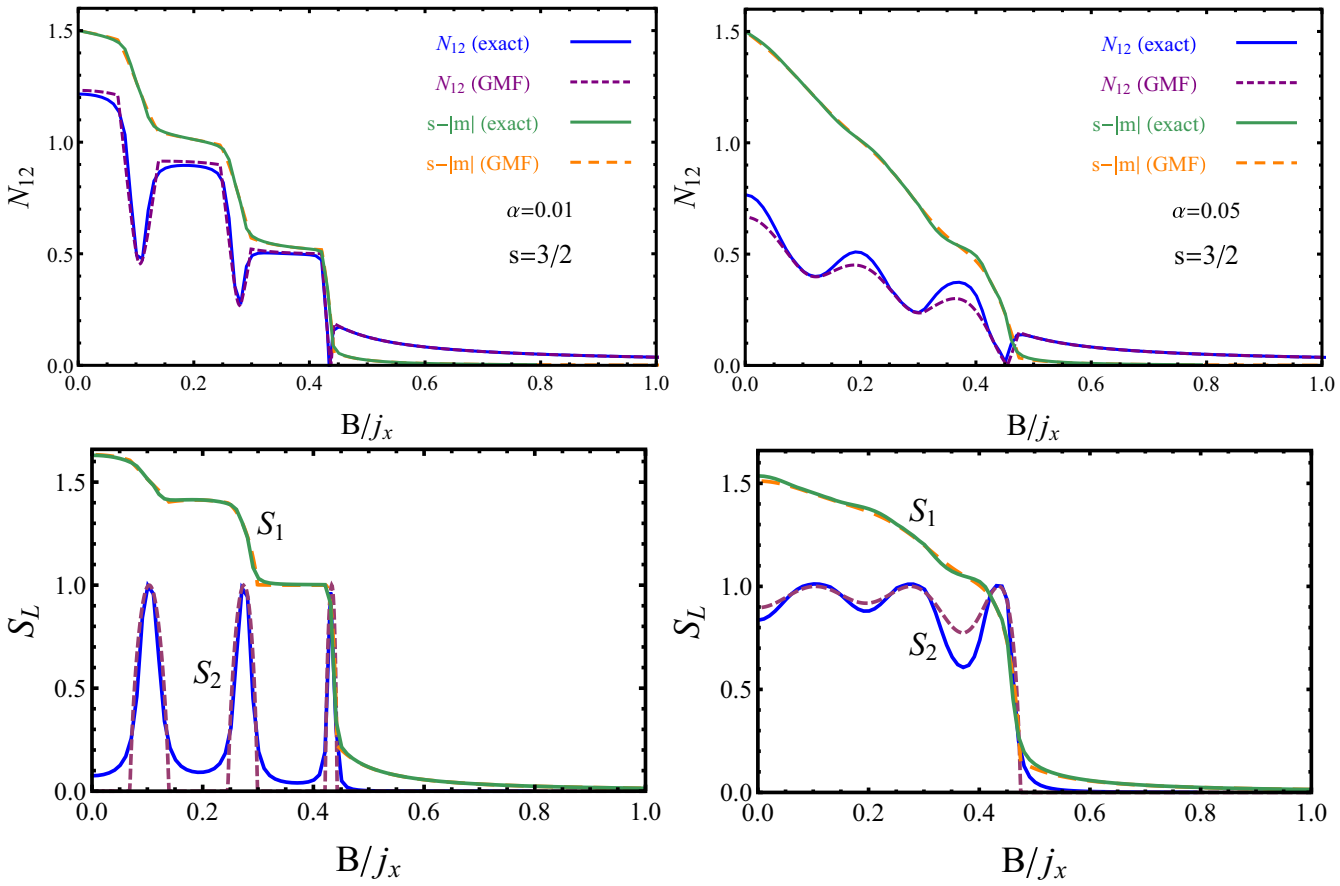

FIG. 6. Top: Exact and GMF results for the negativity in the dimerized spin-3/2 chain as a function of the (scaled) magnetic field, for two different values of the coupling factor α. Again, $m = \langle S_z \rangle / n$ denotes the intensive magnetization. Bottom: The corresponding exact (solid lines) and GMF (dashed lines) results for the entanglement entropies of a strongly coupled spin pair (S_2) and a single spin (S_1), with the rest of the chain, as a function of the (scaled) magnetic field in the $s = 3/2$ chain for the previous values of α.

$b_i^\dagger$ bosonic operators ($[b_i, b_j^\dagger] = \delta_{ij}$), while around the parity-breaking mean field a similar replacement is to be applied to the rotated spin operators $S_i^{z'}$, $S_i^{\pm'}$, with $S_i^{-'}|\Theta\rangle = 0$. Taking into account parity restoration effects, such bosonization leads to the analytic expression

$$N_{12} = \begin{cases} f + \sqrt{f(f+1)}, & |B| > B_c = J_x s \\ 2[f + \sqrt{f(f+1)}] + 1/2, & |B| < B_c, \end{cases} \tag{21}$$

where f is the average single-site bosonic occupation number,

$$f = \frac{1}{2}\left(\sqrt{1 + \frac{\lambda^2 - \omega_m^2}{\omega_+ \omega_-}} - 1\right), \tag{22}$$

with $\lambda = |B|$ (B_c) for $|B| > B_c$ ($< B_c$), $\omega_m = \frac{\omega_+ + \omega_-}{2}$, and $\omega_\pm$ the bosonic eigenfrequencies

$$\omega_\pm = \begin{cases} B_c\sqrt{(1 \pm (B/B_c)^2)(1 \pm \chi)}, & |B| < B_c \\ B_c\sqrt{(B/B_c \pm 1)(B/B_c \pm \chi)}, & |B| > B_c \end{cases}. \tag{23}$$

The exact results for the negativity are verified to approach the previous finite and s-independent bosonic limit for large spin in the anisotropic case $\chi < 1$ (bottom-left panel in Fig. 7). The corresponding pair entanglement entropy is given by $S_2 = -f \log_2 f + (f+1)\log_2(f+1) + \delta$, where $\delta = 0$ (1) for $B > B_c$ ($< B_c$) [32].

However, in the XX case $\chi = 1$ ($J_y = J_x$) the behavior for high spin is different. Here H_{12} commutes with the total spin component $S_t^z = S_1^z + S_2^z$, implying that the parity-breaking solution of the pair mean field is actually breaking a continuous symmetry. Symmetry restoration implies then integration over all rotations around the z axis (i.e., projection onto definite magnetization) and the previous approach [Eqs. (20)–(21)] no longer holds. Nevertheless, since the exact GS has now definite magnetization M, it is of the form

$$|\psi_M\rangle = \sum_{m=-s}^{M+s} \alpha_M^m |m, M-m\rangle, \quad (\chi = 1), \tag{24}$$

for $M \leqslant 0$, with M determined by the applied transverse field ($M \approx -2s[B/B_c]$ for $B \leqslant B_c$, $[\ldots]$ integer part) and all α_M^m of the same sign for $J_x > 0$ in (1). Equation (24) is directly its Schmidt decomposition, implying that the single-spin reduced state will have eigenvalues $|\alpha_M^m|^2$, twofold degenerate for $m \neq M/2$ ($\alpha_M^m = \alpha_M^{M-m}$), leading to the entanglement spectrum of the top-right panel in Fig. 7. The number of nonzero eigenvalues (the Schmidt rank of $|\psi_M\rangle$) will then be $2s + 1 - |M|$. For $|M|$ not too close to $2s$ the coefficients will have essentially a *Gaussian distribution*, as shown in the

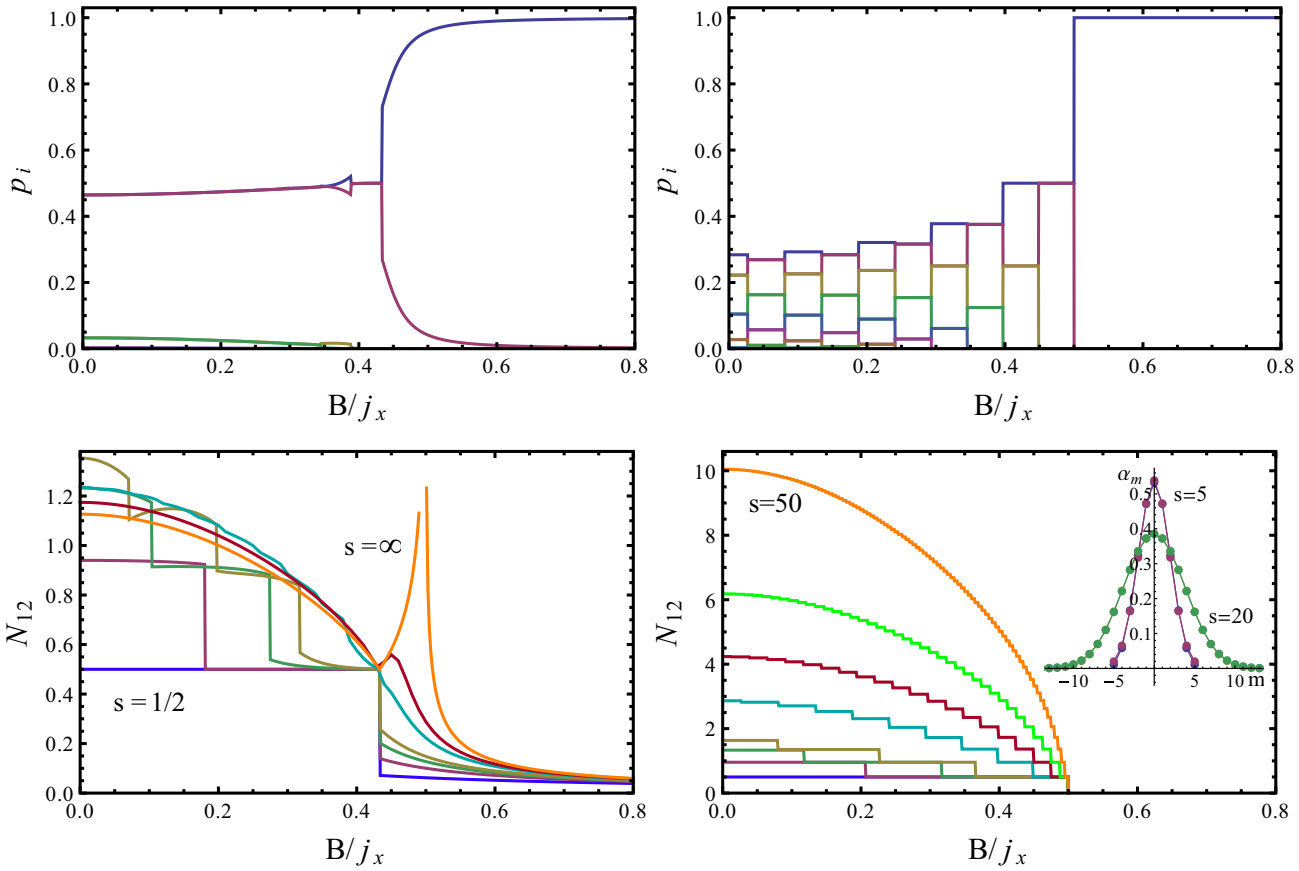

FIG. 7. Top: The entanglement spectrum of the GS of a spin-s pair as a function of the applied field for $s = 5$ and $\chi = J_y/J_x = 0.75$ (left) and 1 (right). In the anisotropic case it is formed essentially by just two degenerate eigenvalues below the factorizing field [as described by Eq. (20)], whereas in the XX case (right) there are several nonvanishing eigenvalues (twofold degenerate), in agreement with the Gaussian profile (25) [shown in the bottom-right panel at $B = 0$ for $s = 5$ and 20, together with the exact results, indistinguishable from (25)]. Bottom: The negativity of the pair as a function of the (scaled) magnetic field for different spin values and $\chi = 0.75$ (left), where $s = 1/2, 1, \frac{3}{2}, 2, 5, 10,$ and ∞ [bosonic limit, Eq. (21)], and $\chi = 1$ (right), where $s = 1/2, 1, \frac{3}{2}, 2, 5, 10, 20,$ and 50. Notice the different scales.

bottom-right panel of Fig. 7,

$$\alpha_M^m \propto e^{-(m-M/2)^2/(4\sigma_M^2)}, \quad \sigma_M^2 \approx r_M s, \tag{25}$$

where for s not too small, the fluctuation $\sigma_M^2 \approx \langle (S_1^z - M/2)^2 \rangle$ will be *proportional to the spin* s, as obtained from the high spin expansion of the exact eigenvector equation. The factor r_M decreases for increasing $|M|$ and for $M = 0$ it is given by $r_0 = 1/(2\sqrt{2}) \approx 0.35$, whereas for $|M| = s/2$, $r_{s/2} \approx 0.32$. The overlap between the Gaussian expression and exact distribution exceeds 0.999 for $s \geqslant 5$ at $M = 0$.

Let us remark that for two spins s coupled to total spin $2s$ and magnetization M, the corresponding distribution of the α_M's are Clebsch-Gordan coefficients, which also lead to a Gaussian distribution for high s and $|M|$ not close to $2s$, with a fluctuation also proportional to s but slightly smaller [at zero field, $\sigma_0^2 \approx s/4 < s/(2\sqrt{2})$]. Hence the actual distribution in the GS of the XX pair contains small admixtures from lower values of the total spin, as H_{12} does not commute with it.

Therefore the negativity of the pair can be estimated through the Gaussian approximation, which leads, using Eq. (10), to

$$N_{12} \approx \sqrt{2\pi\sigma_M^2} - \tfrac{1}{2} \approx \sqrt{2\pi r_M s} - \tfrac{1}{2}. \tag{26}$$

Consequently, the entanglement is *unbounded* for increasing spin, with N_{12} increasing as $\sqrt{s}$ for $\chi = 1$, as verified in the bottom-right panel of Fig. 7 and in Fig. 8. The entanglement entropy of the pair becomes, similarly, $S(\rho_1) \approx \frac{1}{2\ln 2}[1 + \ln(2\pi\sigma_M^2)] \approx \frac{1}{2\ln 2}[1 + \ln(2\pi r_M s)]$.

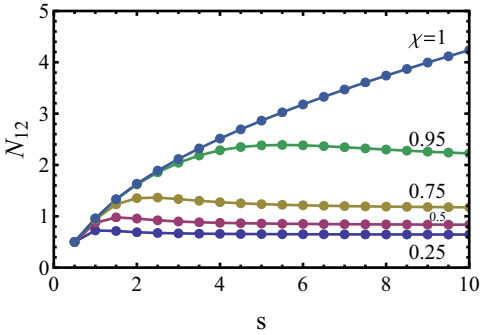

FIG. 8. Negativity of a pair for increasing spin s at zero field for different anisotropies $\chi = J_y/J_x$. For $\chi < 1$ they saturate, approaching the limit values (21), while for $\chi = 1$ they increase as $\sqrt{s}$, as given by Eq. (26) (indistinguishable from the exact result for $s \geqslant 1$ on this scale).

The previous behavior of the pair entanglement with s holds also for an XXZ coupling $-J(S_1^x S_2^x + S_1^y S_2^y) - J_z S_1^z S_2^z$ if $J > J_z > -J$ ($J > 0$), in which case the coefficients α_M^m remain Gaussian with finite width σ_M. However, in the AFM case $J_z = -J$, $J > 0$ (equivalent through local rotations to $J_z = J < 0$) at zero magnetization, the Gaussian becomes uniform and the pair GS becomes *maximally entangled*, i.e., $|\alpha_m^0| = 1/\sqrt{2s+1}\ \forall\ m$ (with $|\psi_0\rangle$ becoming the singlet state with zero total angular momentum for $J_z = J < 0$). Such a state leads then to $N_{12} = s$ and $S(\rho_1) = \log_2(2s+1)$, with maximum fluctuation $\langle S_1^{z\,2}\rangle = s(s+1)/3$.

IV. CONCLUSIONS

We have shown that entanglement and magnetization in dimerized spin-s XY chains immersed in a transverse field can exhibit a nontrivial behavior for weak coupling between pairs, which lies obviously beyond the scope of a conventional MF description. However, they can be correctly described and understood by means of a self-consistent *pair* mean-field approach. Such an approach predicts up to $2s$ dimerized phases for increasing values of the applied field below the pair factorizing field, if the coupling α is sufficiently small and $J_y/J_x > 0$, characterized by decreasing values of the pair entanglement and lying between parity-breaking phases. Dimerized sectors are visible in the exact results through approximate plateaus in the pair negativity N_{12} and chain magnetization, and the low values of the pair entanglement S_2 with the rest of the chain, while the intermediate parity-breaking phases through the minima in N_{12} and maxima in S_2, together with the linear increase in the magnetization. The latter was also seen to correlate with the entanglement entropy S_1 of a single spin, which is here larger than S_2 except in the vicinity of the factorizing field.

These effects can be all reproduced by the pair MF if symmetry restoration is employed in parity-breaking phases. These multiple phases arise below increasingly lower values of the coupling between pairs as s increases, with the XX case being more favorable. Nonmonotonous magnetic behavior of N_{12} and S_2 nevertheless persists for higher values, in agreement with that of the parity-breaking parameter of the pair MF. We have also shown that the pair MF improves conventional MF also for stronger couplings, providing a good prediction of the pair negativity (which vanishes identically in conventional MF) for all α, including the uniform limit $\alpha = 1$.

It was shown as well that the isolated pair GS negativity rapidly saturates as s increases in the anisotropic XY case, in agreement with the predictions of a MF plus RPA treatment for the pair. However, in the XX case it increases as $s^{1/2}$, due to the Gaussian-like distribution (of width $\propto s^{1/2}$) of the Schmidt coefficients, being then intermediate between the XY and the full AFM case.

These results indicate that interesting nontrivial phases can arise in spin-s systems for nonhomogeneous couplings, which can be predicted by generalized MF approaches based on suitable nontrivial units like pairs or clusters. While treating the internal couplings exactly, they can also account for nonperturbative effects of the coupling between units through symmetry breaking. In principle, they can be easily implemented in more complex situations (nonuniform fields, higher dimensions, etc.), enabling exploration of the basic physics of such systems and offering a convenient starting point for more involved or specific treatments.

ACKNOWLEDGMENTS

The authors acknowledge support from CONICET (A.B., N.C., J.M.M.) and CIC (R.R.) of Argentina. Work supported by CONICET through PIP Grant No. 112201501-00732.

[1] L. Amico, R. Fazio, A. Osterloh, and V. Vedral, Rev. Mod. Phys. **80**, 517 (2008).
[2] J. Eisert, M. Cramer, and M. B. Plenio, Rev. Mod. Phys. **82**, 277 (2010).
[3] T. J. Osborne and M. A. Nielsen, Phys. Rev. A **66**, 032110 (2002).
[4] G. Vidal, J. I. Latorre, E. Rico, and A. Kitaev, Phys. Rev. Lett. **90**, 227902 (2003).
[5] M. A. Nielsen and I. L. Chuang, *Quantum Computation and Quantum Information* (Cambridge University Press, Cambridge, UK, 2000).
[6] S. Haroche and J. M. Raimond, *Exploring the Quantum: Atoms, Cavities and Photons* (Oxford University Press, Oxford, UK, 2006).
[7] D. Porras and J. I. Cirac, Phys. Rev. Lett. **92**, 207901 (2004).
[8] I. M. Georgescu, S. Ashhab, and F. Nori, Rev. Mod. Phys. **86**, 153 (2014).
[9] R. Blatt and C. F. Roos, Nat. Phys. **8**, 277 (2012).
[10] C. Senko, P. Richerme, J. Smith, A. Lee, I. Cohen, A. Retzker, and C. Monroe, Phys. Rev. X **5**, 021026 (2015).
[11] R. Barends *et al.*, Nature (London) **534**, 222 (2016); R. Barends, J. Kelly, A. Megrant, D. Sank, E. Jeffrey, Y. Chen, Y. Yin, B. Chiaro, J. Mutus, C. Neill, P. O'Malley, P. Roushan, J. Wenner, T. C. White, A. N. Cleland, and J. M. Martinis, Phys. Rev. Lett. **111**, 080502 (2013).
[12] M. Lewenstein, A. Sanpera, and V. Ahufinger, *Ultracold Atoms in Optical Lattices* (Oxford University Press, Oxford, UK, 2012).
[13] V. Ohanyan, O. Rojas, J. Strečka, and S. Bellucci, Phys. Rev. B **92**, 214423 (2015).
[14] C. K. Majundar and D. K. Gosh, J. Math. Phys. **10**, 1388 (1969); **10**, 1399 (1969); B. S. Shastry and B. Sutherland, Phys. Rev. Lett. **47**, 964 (1981).
[15] H. J. Schmidt, J. Phys. A: Math. Gen. **38**, 2123 (2005).
[16] J. H. H. Perk, H. W. Capel, M. J. Zuilhof, and Th. J. Siskens, Phys. A **81**, 319 (1975); Th. J. Siskens, H. W. Capel, and J. H. H. Perk, Phys. Lett. A **53**, 21 (1975).
[17] J. H. H. Perk, H. W. Capel, and Th. J. Siskens, Physica A **89**, 304 (1977); J. H. H. Perk and H. W. Capel, *ibid.* **92**, 163 (1978); J. H. H. Perk and H. Au-Yang, J. Stat. Phys. **135**, 599 (2009).
[18] E. I. Kutznetsova and E. B. Fel'dman, JETP Lett. **102**, 882 (2006); E. B. Fel'dman and M. G. Rudavets, *ibid.* **81**, 47 (2005); S. I. Doronin, A. N. Pyrkov, and E. B. Fel'dman, *ibid.* **85**, 519 (2007).

[19] D. Kaszlikowski, W. Son, and V. Vedral, Phys. Rev. A **76**, 054302 (2007).
[20] J. Sirker, A. Herzog, A. M. Oles, and P. Horsch, Phys. Rev. Lett. **101**, 157204 (2008); A. Herzog, P. Horsch, A. M. Oles, and J. Sirker, Phys. Rev. B **84**, 134428 (2011).
[21] V. Karimipour and L. Memarzadeh, Phys. Rev. B **77**, 094416 (2008).
[22] S. Rachel, Europhys. Lett. **86**, 37005 (2009).
[23] F. Michaud, F. Vernay, S. R. Manmana, and F. Mila, Phys. Rev. Lett. **108**, 127202 (2012).
[24] P. Merchant, B. Normand, K. W. Kramer, M. Boehm, D. F. McMorrow, and Ch. Rüegg, Nat. Phys. **10**, 373 (2014).
[25] M.-G. Hu, K. Xue, and M.-L. Ge, Phys. Rev. A **78**, 052324 (2008).
[26] G. L. Giorgi, Phys. Rev. B **79**, 060405(R) (2009); **80**, 019901(E) (2009).
[27] N. Canosa, R. Rossignoli, and J. M. Matera, Phys. Rev. B **81**, 054415 (2010).
[28] C. A. Lamas and J. M. Matera, Phys. Rev. B **92**, 115111 (2015); J. M. Matera and C. A. Lamas, J. Phys.: Condens. Matter **26**, 326004 (2014).
[29] A. Boette, R. Rossignoli, N. Canosa, and J. M. Matera, Phys. Rev. B **91**, 064428 (2015).
[30] T. Ramos, H. Pichler, A. J. Daley, and P. Zoller, Phys. Rev. Lett. **113**, 237203 (2014); A. W. Glaetzle, M. Dalmonte, R. Nath, C. Gross, I. Bloch, and P. Zoller, *ibid.* **114**, 173002 (2015); I. Bloch, J. Dalibard, and W. Zwerger, Rev. Mod. Phys. **80**, 885 (2006).
[31] E. Lieb, T. Schultz, and D. Mattis, Ann. Phys. (NY) **16**, 407 (1961).
[32] J. M. Matera, R. Rossignoli, and N. Canosa, Phys. Rev. A **82**, 052332 (2010).
[33] J. Kurmann, H. Thomas, and G. Müller, Physica A (Amsterdam, Neth.) **112**, 235 (1982).
[34] R. Rossignoli, N. Canosa, and J. M. Matera, Phys. Rev. A **77**, 052322 (2008).
[35] R. Rossignoli, N. Canosa, and J. M. Matera, Phys. Rev. A **80**, 062325 (2009).
[36] G. Vidal and R. F. Werner, Phys. Rev. A **65**, 032314 (2002).
[37] K. Zyczkowski, P. Horodecki, A. Sanpera, and M. Lewenstein, Phys. Rev. A **58**, 883 (1998); K. Zyczkowski, *ibid.* **60**, 3496 (1999).
[38] R. F. Werner, Phys. Rev. A **40**, 4277 (1989).